Universität Stuttgart

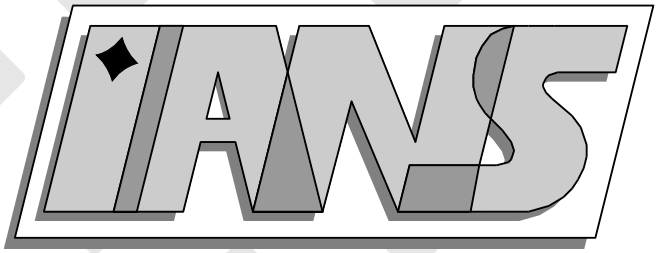

Mortar Finite Elements for Interface Problems

Bishnu P. Lamichhane, Barbara I. Wohlmuth

Berichte aus dem Institut für Angewandte Analysis und Numerische Simulation

Preprint 2003/001

Universität Stuttgart

Mortar Finite Elements for Interface Problems

Bishnu P. Lamichhane, Barbara I. Wohlmuth

Berichte aus dem Institut für Angewandte Analysis und Numerische Simulation

Preprint 2003/001

Institut für Angewandte Analysis und Numerische Simulation (IANS)
Fakultät Mathematik und Physik
Fachbereich Mathematik
Pfaffenwaldring 57
D-70 569 Stuttgart

E-Mail: ians-preprints@mathematik.uni-stuttgart.de
WWW: http://preprints.ians.uni-stuttgart.de

ISSN **1611-4176**

Abstract

Mortar techniques provide a flexible tool for the coupling of different discretization schemes or triangulations. Here, we consider interface problems within the framework of mortar finite element methods. We start with the saddle point formulation and show that the interface conditions enter in the right hand side. Using dual Lagrange multipliers, we can work with scaled sparse matrices, and static condensation gives rise to a symmetric and positive definite system on the unconstrained product space. The iterative solver is based on a modified multigrid approach. Numerical results illustrate the performance of our approach.

Key words. mortar finite elements, Lagrange multiplier, saddle point problem, domain decomposition, interface problem, non-matching triangulation
AMS subject classifications. 65N30, 65N55

1 Introduction

Domain decomposition techniques provide powerful tools for the coupling of different discretization schemes or of non-matching triangulations. Non-matching triangulations are of interest, for example, if different subdomains are meshed independently, or if adaptive remeshing is done in some subdomains. This can be caused by discontinuous diffusion coefficients, problems with transmission conditions at the interface, local anisotropies, singular sources or corner singularities. Here, we consider mortar finite elements for interface problems. Such interface problems arise in different situations, for example, in heat conduction in composite materials or in problems with transmission conditions at the interfaces and discontinuous sources. The characteristic idea of mortar methods is to decompose the domain of interest in non-overlapping subdomains and to replace the strong pointwise continuity at the interfaces by a weak integral condition. There are two equivalent variational formulations. The first one results in a positive definite system on the constrained mortar space [5, 6], and the second one gives rise to an indefinite system associated with the unconstrained product space and the Lagrange multiplier space [4]. Here, we follow the saddle point approach and rewrite the interface problem as indefinite variational equation. We consider non-homogeneous jumps in the flux and in the solution. Compared to standard formulations for the Laplace operator, we have to include two additional terms reflecting the interface conditions. The jump terms enter only in the right hand side, and the arising stiffness matrix does not depend on the interface conditions.

Conforming finite element methods for elliptic problems with discontinuous coefficients and homogeneous interface conditions are addressed in [1]. Finite element methods for non-homogeneous elliptic interface problems are analyzed in [8], and it is shown that the discretization error is of optimal order for linear finite elements on quasi-uniform triangulations. A survey on non-overlapping domain decomposition methods for elliptic interface problems can be found in [20]. A Least-squares finite element method for elliptic interface problems with Dirichlet and Neumann boundary data is proposed and analyzed in [9]. In particular, error estimates for non-matching triangulations at the interface are given. Elliptic and parabolic interface problems with non-zero jump in the flux across the smooth interface are considered in [10, 13]. In [10], nearly optimal error estimates in the energy-norm and in the L^2-norm are established under reasonable regularity assumptions on the original solutions, whereas some new a priori estimates are presented in [13]. The immersed interface method

is based on using the jumps in the solution and its derivative in finite difference schemes modifying the standard schemes in the neighborhood of the interface, see [14]. The idea to precondition the elliptic equation before using the immersed interface method is proposed in [15] resulting in a fast algorithm for elliptic equations with large jumps in the coefficients. An extension of the immersed interface method to boundary value problems on irregular domains with Neumann and Dirichlet boundary conditions can be found in [17]. The immersed interface method with a finite element formulation is considered in [16]. Nitsche techniques provide flexible domain decomposition techniques and have been successfully used for the numerical approximation of partial differential equations, see, e.g., [3, 12]. The analysis of the discretization scheme is restricted to homogeneous interface conditions, and optimal a priori estimates are given. A similar approach can be found in [11], where a stationary heat conduction problem in two dimensions with a discontinuous conducting coefficient across a smooth interface is considered. Optimal a priori estimates for appropriately modified piecewise linear elements on a non-degenerate triangulation have been established. Mortar methods based on dual Lagrange multiplier spaces for elliptic problems are considered in [18]. Here, we propose a similar approach based on mortar techniques and Lagrange multipliers. We consider non-homogeneous jumps in the flux and in the solution across the interface. We start with a saddle point formulation of the interface problem. Our approach is quite flexible and can easily be applied to general type of elliptic interface problems, where the interface and the interface conditions are a priori known. Here, we focus on dual Lagrange multiplier spaces. In terms of the biorthogonality between the nodal basis functions of our Lagrange multiplier space and the finite element trace space, we get a diagonal mass matrix on the slave side. As a consequence, we can locally eliminate the Lagrange multiplier from the saddle point formulation and obtain a positive definite algebraic system.

The paper is organized as follows: In the rest of this section, we present our model interface problem and introduce its saddle point formulation. In Section 2, we briefly outline the mortar discretization scheme and establish a priori estimates for the discretization errors. In Section 3, we consider the algebraic formulation of the saddle point problem in more detail. Local modifications are carried out to obtain a positive definite system for which we can use multigrid methods. Finally in Section 4, we show some numerical results illustrating the performance of our approach. In particular, we give the discretization errors in the L^2-, H^1- and a weighted Lagrange multiplier norm.
Let us consider a bounded polygonal domain $\Omega \subset \mathbb{R}^2$, which is decomposed into two non-overlapping subdomains Ω_1 and Ω_2 with the common interior interface Γ, $\bar{\Gamma} := \partial\Omega_1 \cap \partial\Omega_2$, and assume that the interface Γ can be written as union of straight lines, see Figure 1. For

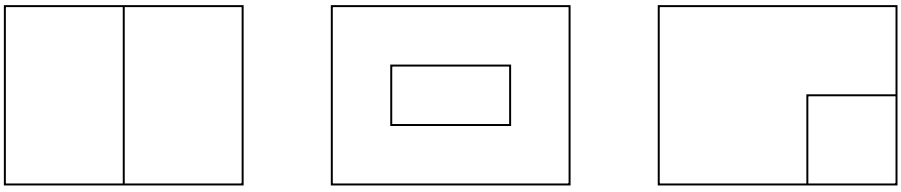

Figure 1: Different decompositions of the domain into two subdomains

simplicity, we restrict ourselves to the case of two subdomains. However, the approach can be generalized to more than two subdomains. We consider the following elliptic second order

boundary value problem on Ω

$$\begin{aligned} -\mathrm{div}(\alpha_1 \nabla u_1) + b_1 u_1 = &\quad f_1, \quad x \in \Omega_1, \\ -\mathrm{div}(\alpha_2 \nabla u_2) + b_2 u_2 = &\quad f_2, \quad x \in \Omega_2, \end{aligned} \tag{1}$$

with homogeneous Dirichlet boundary conditions on $\partial\Omega$. Here, α_1 and α_2 are symmetric and locally constant positive-definite second order tensors specifying the diffusion in the two subdomains. Furthermore, we assume that $f_i \in L^2(\Omega_i)$ and $0 \leq b_i \in L^\infty(\Omega_i), i = 1, 2$. The jump conditions at the interface Γ are given by

$$[u] := u_1 - u_2 \quad = \quad g_D, \quad \text{on} \quad \Gamma, \tag{2}$$

$$[u]_n := (\alpha_1 \nabla u_1) \cdot n_1 + (\alpha_2 \nabla u_2) \cdot n_2 \quad = \quad g_N, \quad \text{on} \quad \Gamma, \tag{3}$$

where n_i is the outward normal on $\partial\Omega_i$. We assume that $g_D \in H^{1/2}_{00}(\Gamma)$ and $g_N \in H^{-1/2}(\Gamma) := \left(H^{1/2}_{00}(\Gamma)\right)'$. On each subdomain, we define

$$H^1_*(\Omega_k) := \{v \in H^1(\Omega_k), v_{|\partial\Omega \cap \partial\Omega_k} = 0\}, \quad k = 1, 2,$$

and consider the unconstrained product space

$$X := H^1_*(\Omega_1) \times H^1_*(\Omega_2).$$

Working with a discretization scheme, we cannot, in general, satisfy the interface conditions (2) and (3) in a strong form. We replace (2) and (3) by a weak variational condition. It is given in terms of the duality pairing on the interface

$$b(v, \mu) := \langle [v], \mu \rangle_\Gamma, \quad v = (v_1, v_2) \in X, \quad \mu \in M := H^{-1/2}(\Gamma).$$

In the rest of this section, we consider the variational formulation of the interface problem. The weak formulation of (1) is obtained by applying Green's formula

$$\begin{aligned} \int_{\Omega_1} (\alpha_1 \nabla u_1) \cdot \nabla \phi_1 \, dx - \int_\Gamma \alpha_1 \nabla u_1 \cdot n_1 \phi_1 \, ds + \int_{\Omega_1} b_1 u_1 \phi_1 \, dx = \int_{\Omega_1} f_1 \phi_1 \, dx, \quad \phi_1 \in H^1_*(\Omega_1), \\ \int_{\Omega_2} (\alpha_2 \nabla u_2) \cdot \nabla \phi_2 \, dx - \int_\Gamma \alpha_2 \nabla u_2 \cdot n_2 \phi_2 \, ds + \int_{\Omega_2} b_2 u_2 \phi_2 \, dx = \int_{\Omega_2} f_2 \phi_2 \, dx, \quad \phi_2 \in H^1_*(\Omega_2). \end{aligned}$$

Taking into account the interface condition for the flux (3), $\alpha_1 \nabla u_1 \cdot n_1 = -\alpha_2 \nabla u_2 \cdot n_2 + g_N$ on Γ, we find for $\phi_i \in H^1_*(\Omega_i)$, $1 \leq i \leq 2$,

$$\begin{aligned} \int_{\Omega_1} (\alpha_1 \nabla u_1) \cdot \nabla \phi_1 \, dx + \int_\Gamma \alpha_2 \nabla u_2 \cdot n_2 \phi_1 \, ds + \int_{\Omega_1} b_1 u_1 \phi_1 \, dx = \int_{\Omega_1} f_1 \phi_1 \, dx + \int_\Gamma g_N \phi_1 \, ds, \\ \int_{\Omega_2} (\alpha_2 \nabla u_2) \cdot \nabla \phi_2 \, dx - \int_\Gamma \alpha_2 \nabla u_2 \cdot n_2 \phi_2 \, ds + \int_{\Omega_2} b_2 u_2 \phi_2 \, dx = \int_{\Omega_2} f_2 \phi_2 \, dx. \end{aligned}$$

The weak formulation of the jump of the solution at the interface can be obtained by multiplying the jump condition (2) with an element of the dual space M. Then the definition of the bilinear form $b(\cdot, \cdot)$ yields

$$b(u, \mu) = \langle g_D, \mu \rangle_\Gamma =: \tilde{g}(\mu), \quad \mu \in M.$$

Introducing the flux λ on Γ by $\lambda := \alpha_2 \nabla u_2 \cdot n_2$, we can write the weak form of (1) as a saddle point problem: Find $(u, \lambda) \in X \times M$ such that

$$\begin{array}{rcll} a(u,v) + & b(v,\lambda) & = & \tilde{f}(v), \qquad v \in X, \\ b(u,\mu) & & = & \tilde{g}(\mu), \qquad \mu \in M, \end{array} \tag{4}$$

where

$$a(u,v) := \sum_{k=1}^{2} \int_{\Omega_k} (\alpha_k \nabla u) \cdot \nabla v \, dx + \int_{\Omega_k} b_k uv \, dx,$$
$$\tilde{f}(v) := \sum_{k=1}^{2} \int_{\Omega_k} f_k v \, dx + \left\langle v_{|\partial\Omega_1}, g_N \right\rangle_\Gamma .$$

The essential points for the existence and the uniqueness of the solution of a saddle point problem are coercivity, continuity and a suitable inf-sup condition. On X, we use the broken H^1-norm

$$\|v\|_{1,\Omega} := \left(\|v\|^2_{1,\Omega_1} + \|v\|^2_{1,\Omega_2} \right)^{1/2},$$

and on M the $H^{-1/2}$-norm. We start with the continuity of the bilinear form $b(\cdot,\cdot)$. By definition, we find

$$b(v,\mu) = \langle [v], \mu \rangle_\Gamma \leq \|[v]\|_{H^{1/2}_{00}(\Gamma)} . \|\mu\|_{H^{-1/2}(\Gamma)}, \quad v \in X, \, \mu \in M.$$

We note that if Γ is a closed curve, see Figure 1, we have $H^{1/2}_{00}(\Gamma) = H^{1/2}(\Gamma)$, and thus

$$\|[v]\|_{H^{1/2}_{00}(\Gamma)} = \|[v]\|_{H^{1/2}(\Gamma)} \leq (\|v_{|\Omega_1}\|_{H^{1/2}(\Gamma)} + \|v_{|\Omega_2}\|_{H^{1/2}(\Gamma)}) \leq C\|v\|_{1,\Omega}.$$

Due to the homogeneous Dirichlet boundary condition imposed on $\partial\Omega$, we find $(v_{|\Omega_i})_{|\Gamma} \in H^{1/2}_{00}(\Gamma)$, $i = 1, 2$, if Γ is not a closed curve. In that case, we can bound

$$\|[v]\|_{H^{1/2}_{00}(\Gamma)} \leq C(\|v_{|\Omega_1}\|_{H^{1/2}(\partial\Omega_1)} + \|v_{|\Omega_2}\|_{H^{1/2}(\partial\Omega_2)}) \leq C\|v\|_{1,\Omega}.$$

As a consequence, we obtain the continuity of the bilinear form $b(\cdot,\cdot)$ on $X \times M$. The bilinear form $a(\cdot,\cdot)$ is continuous on $X \times X$ and coercive on $Y \times Y$, where $Y := \{v \in X, \quad \int_\Gamma [v] d\sigma = 0\}$. As it is standard, we associate a linear operator B with the bilinear form $b(\cdot,\cdot)$ such that

$$B : X \longrightarrow H^{1/2}_{00}(\Gamma) \quad \text{with} \quad Bu \longrightarrow [u].$$

Observing that $\ker B = H^1_0(\Omega) \subset Y$, the coercivity of $a(\cdot,\cdot)$ on $\ker B \times \ker B$ is guaranteed. To see that the inf-sup condition holds, we start with the definition of the dual norm

$$\|\mu\|_{H^{-1/2}(\Gamma)} := \sup_{v \in H^{1/2}_{00}(\Gamma)\setminus\{0\}} \frac{\langle v, \mu \rangle_\Gamma}{\|v\|_{H^{1/2}_{00}(\Gamma)}}.$$

Each $v \in H^{1/2}_{00}(\Gamma)$ can be extended by zero on $\partial\Omega_2 \backslash \Gamma$ to a function in $H^{1/2}(\partial\Omega_2)$, still denoted by v. Using the harmonic extension $\mathcal{H}v$ of v to Ω_2, we have $\|\mathcal{H}v\|_{1,\Omega_2} \leq C\|v\|_{H^{1/2}_{00}(\Gamma)}$.

Now, we define a function $\tilde{v} \in X$ as $\tilde{v}_{|\Omega_1} := 0$ and $\tilde{v}_{|\Omega_2} := \mathcal{H}v$, and we get $\|\tilde{v}\|_{1,\Omega} \leq C\|v\|_{H_{00}^{1/2}(\Gamma)}$. This yields

$$\|\mu\|_{H^{-1/2}(\Gamma)} = \sup_{v \in H_{00}^{1/2}(\Gamma)\setminus\{0\}} \frac{\langle v, \mu\rangle_\Gamma}{\|v\|_{H_{00}^{1/2}(\Gamma)}} \leq C \sup_{\tilde{v}\in X\setminus\{0\}} \frac{b(\tilde{v}, \mu)}{\|\tilde{v}\|_{1,\Omega}}.$$

Hence, the variational problem (4) has a unique solution.

2 Mortar discretizations and a priori error estimates

In this section, we briefly review mortar finite elements and prove optimal a priori estimates for the discretization errors. Let $\mathcal{T}_{h_1}$ and $\mathcal{T}_{h_2}$ be independent shape regular simplicial triangulations on Ω_1 and Ω_2, respectively and $h := \max_{K\in\mathcal{T}_{h_1}\cup\mathcal{T}_{h_2}} h_K$, where h_K is the diameter of an element K. The interface Γ is associated with a one-dimensional triangulation inherited either from the triangulation on Ω_1 or on Ω_2. Without loss of generality, the interface Γ inherits its one-dimensional mesh from $\mathcal{T}_{h_2}$. The side of Γ associated with Ω_2 is called slave side and the one associated with Ω_1 master side. We denote by $\mathcal{T}_\Gamma$ the triangulation on Γ whose elements are boundary edges of $\mathcal{T}_{h_2}$. The unconstrained discrete finite element space is denoted by

$$X_h := \mathcal{S}^p(\Omega_1, \mathcal{T}_{h_1}) \times \mathcal{S}^p(\Omega_2, \mathcal{T}_{h_2}),$$

where $\mathcal{S}^p(\Omega_k, \mathcal{T}_{h_k})$ stands for the space of linear ($p = 1$) or quadratic ($p = 2$) conforming finite elements in the subdomain Ω_k associated with the triangulation $\mathcal{T}_{h_k}$ and satisfies homogeneous Dirichlet boundary conditions on $\partial\Omega_k \cap \partial\Omega$, $k = 1, 2$. We note that no interface condition is imposed on X_h, and the elements in X_h do not have to satisfy a continuity condition at the interface. Let W_h be the trace space of finite element basis functions from the slave side, i.e., of $S^p(\Omega_2, \mathcal{T}_{h_2})$, restricted to Γ. Due to the homogeneous boundary conditions on $\partial\Omega$, we find $W_h \subset H_{00}^{1/2}(\Gamma)$. To satisfy a suitable discrete inf-sup condition, we use a discrete Lagrange multiplier space such that $\dim M_h \leq \dim W_h$. A natural and efficient choice for the construction of a good Lagrange multiplier space is to define its basis functions locally and to associate them with the interior nodes of the slave side. We observe that although $u \in H^{p+1}(\Omega_2)$, λ is, in general, not an element in $H^{p-1/2}(\Gamma)$. This is due to the fact that the normal has jumps if Γ has corners. Therefore, we decompose Γ into a finite number of straight segments γ_l, $1 \leq l \leq M$, and work with the Lagrange multiplier spaces defined on γ_l. Hence, we can write

$$\bar{\Gamma} = \bigcup_{l=1}^{M} \bar{\gamma}_l,$$

where $\gamma_k \cap \gamma_l = \emptyset$, and $\bar{\gamma}_k \cup \bar{\gamma}_l$ is not a straight line, $1 \leq k \neq l \leq M$. In the examples given in Figure 1, we find $M = 1$, $M = 4$ and $M = 2$ (from the left to the right). We remark that we use the decomposition of Γ into straight lines for the definition of the discrete Lagrange multiplier space, but that we work with the $H_{00}^{1/2}$-norm on Γ. In contrast to the general mortar framework, we do not use the $H_{00}^{1/2}$-norm on γ_l, $1 \leq l \leq M$. Now, we denote by $W_h(\gamma_l)$, the trace of $S^p(\Omega_2, \mathcal{T}_{h_2})$ restricted to γ_l, and we set $W_{0;h}(\gamma_l) := H_0^1(\gamma_l) \cap W_h(\gamma_l)$. Our discrete Lagrange multiplier space is defined as the product space

$$M_h := \prod_{l=1}^{M} M_h(\gamma_l),$$

where $\dim M_h(\gamma_l) = \dim W_{0;h}(\gamma_l)$. Let us denote the nodal basis functions in $W_{0;h}(\gamma_l)$, associated with the one-dimensional mesh on the slave side by $\{\varphi_i^l\}_{1\le i\le n_s^l}$, $n_s^l := \dim W_{0;h}(\gamma_l)$. We use dual Lagrange multiplier spaces defined in [18]. Then, the basis functions $\{\mu_i^l\}_{1\le i\le n_s^l}$ of $M_h(\gamma_l)$ satisfy the following biorthogonality relation

$$\int_{\gamma_l} \mu_i^l \, \varphi_j^l \, d\sigma = \delta_{ij} \int_{\gamma_l} \varphi_j^l \, d\sigma \quad , \quad 1 \le i, j \le n_s^l,$$

and we have $\sum_{i=1}^{n_s^l} \mu_i^l = 1$ on γ_l. Furthermore for $p = 2$, the linear hat functions are contained in the Lagrange multiplier space. To establish a priori estimates for the discretization errors, we consider the saddle point formulation (4) of the interface problem and apply the theory of mixed finite elements. Replacing the space $X \times M$ by our discrete space $X_h \times M_h$ in (4), we obtain our discrete variational problem: Find $(u_h, \lambda_h) \in X_h \times M_h$ such that

$$\begin{array}{lcll} a(u_h, v) + b(v, \lambda_h) & = & \tilde{f}(v), & v \in X_h, \\ b(u_h, \mu) & = & \tilde{g}(\mu), & \mu \in M_h. \end{array} \tag{5}$$

Since $X_h \subset X$ and $M_h \subset M$, we get the continuity of the bilinear form $a(\cdot,\cdot)$ on $X_h \times X_h$ and of $b(\cdot,\cdot)$ on $X_h \times M_h$. Observing $\ker B_h := \{v_h \in X_h | \quad b(v_h, \mu) = 0,\ \mu \in M_h\} \subset Y$, we obtain the coercivity of $a(\cdot,\cdot)$ on $\ker B_h \times \ker B_h$. To establish the discrete inf-sup condition, we introduce $\tilde{W}_h \subset W_h$ with $\dim \tilde{W}_h = \dim M_h$. The basis functions $\tilde{\varphi}_i$ of $\tilde{W}_h$ are associated with the interior nodes of γ_l. If x_i is a node adjacent to an endpoint $x_j \in \Omega$ of some γ_l, we define $\tilde{\varphi}_i := \varphi_i + \frac{1}{2}\varphi_j$, and for all other nodes, we set $\tilde{\varphi}_i := \varphi_i$, where φ_i denotes the standard nodal basis function of W_h. Here, we assume that there are at least two nodes between two crosspoints. The basis functions of $\tilde{W}_h$ in the linear case are shown in the left picture of Figure 2, and the dual Lagrange multiplier basis functions are shown in the right picture. The basis functions are associated with the filled circles.

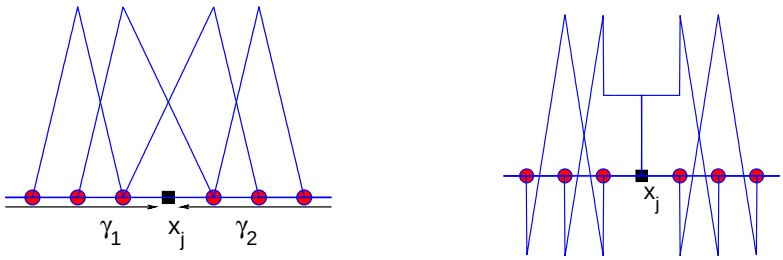

Figure 2: Basis functions of $\tilde{W}_h$ (left) and of M_h (right)

Now, we define two quasi-projection operators Q and Q^* by

$$\begin{array}{lll} & Q : L^2(\Gamma) \longrightarrow \tilde{W}_h, & \int_\Gamma Qv\, \mu_h \, d\sigma = \int_\Gamma v\, \mu_h \, d\sigma, \qquad \mu_h \in M_h, \\ \text{and} & Q^* : L^2(\Gamma) \longrightarrow M_h, & \int_\Gamma Q^* v\, w_h \, d\sigma = \int_\Gamma v\, w_h \, d\sigma, \qquad w_h \in \tilde{W}_h. \end{array}$$

The biorthogonality of $M_h(\gamma_l)$ and $W_{0;h}(\gamma_l)$ and the modification of $\tilde{\varphi}_i$ at the vertices adjacent to a crosspoint yield

$$\int_\Gamma \tilde{\varphi}_i \mu_k \, d\sigma = \delta_{ik} \int_\Gamma \varphi_i \, d\sigma + \sum_{j \in \mathcal{N}_c} \frac{c_{ij}}{2} \int_\Gamma \varphi_j \mu_k \, d\sigma,$$

where $\mathcal{N}_c$ is the set of crosspoints and $c_{ij} = 1$ if the node x_i is adjacent to the crosspoint x_j and otherwise $c_{ij} = 0$. Thus, the operators are well-defined. The associated mass matrices are block diagonal and the block size does not depend on the meshsize. As a consequence, the action of Q and Q^* can be computed locally. Moreover, it is easy to see that $Qv = v, v \in \tilde{W}_h$ and $\|Qv\|_{0,\Gamma} \leq C\|v\|_{0,\Gamma}$, and that $Q^*v = v, v \in M_h$ and $\|Q^*v\|_{0,\Gamma} \leq C\|v\|_{0,\Gamma}$. We denote by P the L^2-projection on $\tilde{W}_h$. In terms of the L^2-stability and an inverse estimate, the $H^{1/2}_{00}$-stability of Q can be shown

$$\|Qv\|_{H^{1/2}_{00}(\Gamma)} \leq \|Qv - Pv\|_{H^{1/2}_{00}(\Gamma)} + \|Pv\|_{H^{1/2}_{00}(\Gamma)} \leq C\left(\frac{1}{\sqrt{h}}\|Qv - Pv\|_{0,\Gamma} + \|v\|_{H^{1/2}_{00}(\Gamma)}\right)$$
$$\leq C\left(\frac{1}{\sqrt{h}}\|v - Pv\|_{0,\Gamma} + \|v\|_{H^{1/2}_{00}(\Gamma)}\right) \leq C\|v\|_{H^{1/2}_{00}(\Gamma)}.$$

In the last step, we have used the approximation property of the projection P. The $H^{1/2}_{00}$-stability of Q guarantees the discrete inf-sup condition

$$\|\mu_h\|_{H^{-1/2}(\Gamma)} = \sup_{v\in H^{1/2}_{00}(\Gamma)\setminus\{0\}} \frac{\int_\Gamma \mu_h\, Qv\, d\sigma}{\|v\|_{H^{1/2}_{00}(\Gamma)}} \leq C \sup_{v\in H^{1/2}_{00}(\Gamma)\setminus\{0\}} \frac{\int_\Gamma \mu_h\, Qv\, d\sigma}{\|Qv\|_{H^{1/2}_{00}(\Gamma)}}$$
$$\leq C \sup_{w_h\in \tilde{W}_h\setminus\{0\}} \frac{\int_\Gamma \mu_h\, w_h\, d\sigma}{\|w_h\|_{H^{1/2}_{00}(\Gamma)}} \leq C \sup_{w_h\in S^p(\Omega_2,\mathcal{T}_{h_2})\setminus\{0\}} \frac{\int_\Gamma \mu_h\, w_h\, d\sigma}{\|w_h\|_{1,\Omega_2}} \leq C \sup_{w_h\in X_h\setminus\{0\}} \frac{b(w_h,\mu_h)}{\|w_h\|_{1,\Omega}}.$$

Here, we have used the extension property $\|\mathcal{H}_h w_h\|_{1,\Omega_2} \leq C\|w_h\|_{H^{1/2}_{00}(\Gamma)}$ of the discrete harmonic extension operator $\mathcal{H}_h$ on $S^p(\Omega_2, \mathcal{T}_{h_2})$. Now, we can apply [7, Theorem III, 4.5] to state

Lemma 1. *The discrete variational problem* (5) *has a unique solution* (u_h, λ_h)*, and there exist two constants* c_1 *and* c_2 *independent of* h *such that*

$$\|u - u_h\|_{1,\Omega} + \|\lambda - \lambda_h\|_{H^{-1/2}(\Gamma)} \leq c_1 \inf_{v_h\in X_h} \|u - v_h\|_{1,\Omega} + c_2 \inf_{\mu_h\in M_h} \|\lambda - \mu_h\|_{H^{-1/2}(\Gamma)}.$$

Now, we consider the two terms of the right hand side in more detail. The best approximation property of X_h is well-known, and we have

$$\inf_{u_h\in X_h} \|u - u_h\|_{1,\Omega} \leq Ch^p(\|u\|^2_{p+1,\Omega_1} + \|u\|^2_{p+1,\Omega_2})^{1/2}, \quad u \in H^{p+1}(\Omega_1) \times H^{p+1}(\Omega_2).$$

To establish the best approximation error of M_h in the $H^{-1/2}$-norm on Γ, we work with Q^*. We denote by P^*_l, the L^2-projection on $M_h(\gamma_l)$. Then, the L^2-stability of Q^* and the best approximation property of $M_h(\gamma_l)$, see [18], yield for $\lambda \in \prod_{l=1}^M H^{p-1/2}(\gamma_l)$,

$$\|\lambda - Q^*\lambda\|^2_{H^{-1/2}(\Gamma)} \leq \sup_{v\in H^{1/2}_{00}(\Gamma)\setminus\{0\}} \frac{\|\lambda - Q^*\lambda\|^2_{0,\Gamma}\|v - Qv\|^2_{0,\Gamma}}{\|v\|^2_{H^{1/2}_{00}(\Gamma)}} \leq Ch\|\lambda - Q^*\lambda\|^2_{0,\Gamma}$$
$$\leq Ch\sum_{l=1}^M \|\lambda - P^*_l\lambda - Q^*(\lambda - P^*_l\lambda)\|^2_{0,\gamma_l} \leq Ch^{2p}\sum_{l=1}^M |\lambda|^2_{H^{p-1/2}(\gamma_l)} \leq Ch^{2p}|u|^2_{p+1,\Omega_2}.$$

Theorem 2. *Under the assumption that* $u \in \prod_{i=1}^2 H^{p+1}(\Omega_i)$*, we have the following a priori estimate for the discretization error*

$$\|u - u_h\|_{1,\Omega} + \|\lambda - \lambda_h\|_{H^{-1/2}(\Gamma)} \leq Ch^p.$$

We note that the a priori estimate cannot be established if we work with a Lagrange multiplier space which is directly defined on Γ.

3 Algebraic formulation

In this section, we consider the algebraic formulation of the saddle point problem (5) and apply a suitable modification to get a positive definite system on the product space. Here and in the following, we use the same notation for the vector representation of the solution and the solution as an element in X_h and M_h. The matrix A is the stiffness matrix associated with the bilinear form $a(\cdot,\cdot)$ on $X_h \times X_h$, and the matrices B and B^T are associated with the bilinear form $b(\cdot,\cdot)$ on $X_h \times M_h$. Then, the algebraic formulation of the saddle point problem is given by

$$\begin{pmatrix} A & B^T \\ B & 0 \end{pmatrix} \begin{pmatrix} u_h \\ \lambda_h \end{pmatrix} = \begin{pmatrix} \tilde{f}_h \\ \tilde{g}_h \end{pmatrix}. \tag{6}$$

Now, we group the degrees of freedom of X_h associated with the interface Γ into two groups $u_{|_\Gamma} := (u_s, u_m)$. The block vector u_s contains all nodal values of u at the interior nodes of γ_l, $1 \le l \le M$, on the slave side, and u_m represents all nodal values of u at the interior nodes of the master side and the nodes at the endpoints $x_e \in \Omega$ of γ_l on the slave side, $1 \le l \le M$, see Figure 3. The associated sets of nodes are called $\mathcal{N}_s$ and $\mathcal{N}_m$. Moreover, $\mathcal{N}_h$ stands for the set of all nodes in X_h, and we set $\mathcal{N}_i := \mathcal{N}_h \backslash (\mathcal{N}_m \cup \mathcal{N}_s)$. The corresponding nodal values in $\mathcal{N}_i$ will be represented by a block vector u_i.

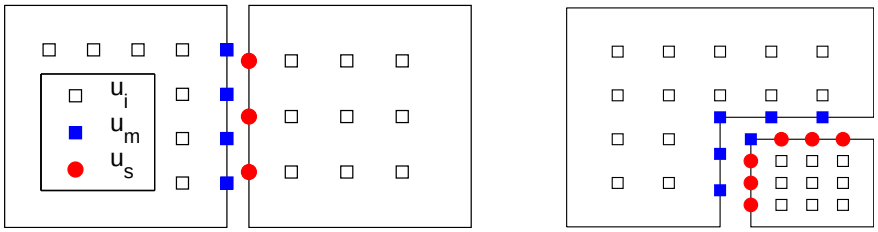

Figure 3: Grouping of the degrees of freedom

Then, the bilinear form $b(\cdot,\cdot)$ restricted to $X_h \times M_h$ written in its algebraic form can be represented by sparse mass matrices

$$M_m u_m + M_s u_s,$$

where the entries of the mass matrices M_s and M_m are given by $(m_s)_{ij} := \int_\Gamma [\phi_j^s]\ \mu_i\, d\sigma$ and $(m_m)_{ij} := \int_\Gamma [\phi_j^m]\ \mu_i\, d\sigma$, respectively. Here, μ_i denotes the basis functions of M_h and ϕ_j^s and ϕ_j^m stand for the nodal basis functions in X_h associated with the nodes in the groups $\mathcal{N}_s$ and $\mathcal{N}_m$, respectively. We remark that $b(\phi_j, \mu) = 0$ for all basis functions $\phi_j \in X_h$ being associated with a node in $\mathcal{N}_i$. The mass matrices are sparse due to the local structure of the supports of the involved basis functions. Using standard Lagrange multipliers, see [5], M_s is a sparse mass matrix with a dense inverse. This observation is our motivation to work with a dual Lagrange multiplier space. In that case, $M_s = D$ is a diagonal matrix. This is due to the fact that we use biorthogonal basis functions for the Lagrange multiplier space. Now, we use the decomposition of the vector u_h into three components $u_h^T = (u_i^T, u_m^T, u_s^T)$, see Figure 3. In terms of this decomposition, we can write the saddle point problem (6) as

$$\begin{pmatrix} A_{ii} & A_{im} & A_{is} & 0 \\ A_{mi} & A_{mm} & A_{ms} & M_m^T \\ A_{si} & A_{sm} & A_{ss} & D \\ 0 & M_m & D & 0 \end{pmatrix} \begin{pmatrix} u_i \\ u_m \\ u_s \\ \lambda_h \end{pmatrix} = \begin{pmatrix} \tilde{f}_i \\ \tilde{f}_m \\ \tilde{f}_s \\ \tilde{g}_h \end{pmatrix}. \tag{7}$$

The algebraic system (7) is indefinite and standard multigrid techniques cannot be applied as easily as for a positive definite system. The given jump in the flux at the interface enters in the right side $\tilde{f}_m$, and the jump in the solution is reflected by $\tilde{g}_h$. We note that in the mortar setting both interface conditions (2) and (3) enter in the right side. Both jump conditions are satisfied in terms of weak integral conditions. Our numerical solution is based on a positive definite system. Following the ideas in [19], we can eliminate λ_h from (7). The third line of the saddle point problem (7) yields

$$\lambda_h = D^{-1}(\tilde{f}_s - A_{si}u_i - A_{sm}u_m - A_{ss}u_s).$$

Only in the case of a dual Lagrange multiplier space, the discrete flux can be eliminated locally. We observe that $\tilde{g}_h$ does not enter here explicitly. Introducing $W^T := \begin{pmatrix} 0 & 0 & D^{-1} \end{pmatrix}$, we can rewrite λ_h in terms of W^T and the defect on the product space

$$\lambda_h = W^T(\tilde{f}_h - Au_h). \tag{8}$$

This observation is the starting point for the modification of the algebraic formulation of the discrete saddle point problem (6). We use the equivalent form $\lambda_h = W^T(\tilde{f}_h - Au_h + AWBu_h) - W^TAW\tilde{g}_h$ of (8) to eliminate λ_h in (6). Shifting the terms $-B^TW^TAW\tilde{g}_h$ and $B^TW^T\tilde{f}_h$ to the right side yields

$$\begin{pmatrix} A & B^T \\ B & 0 \end{pmatrix} \begin{pmatrix} \mathrm{Id} \\ W^TA(WB - \mathrm{Id}) \end{pmatrix} u_h = \begin{pmatrix} (\mathrm{Id} - B^TW^T)\tilde{f}_h + B^TW^TAW\tilde{g}_h \\ \tilde{g}_h \end{pmatrix}. \tag{9}$$

We note that the jump in the trace enters now in both block components on the right side. The system (9) has more equations than unknowns. To obtain a positive definite system for u_h on the product space, we restrict the space of test functions. Assuming that the test function (v_h, μ_h) has the form $(v_h, W^TA(WB - \mathrm{Id})v_h)$, we get

$$\tilde{A}u_h := (\mathrm{Id}, (B^TW^T - \mathrm{Id})AW) \begin{pmatrix} A & B^T \\ B & 0 \end{pmatrix} \begin{pmatrix} \mathrm{Id} \\ W^TA(WB - \mathrm{Id}) \end{pmatrix} u_h = \\ \begin{pmatrix} (\mathrm{Id} - B^TW^T)\tilde{f}_h + (2B^TW^T - \mathrm{Id})AW\tilde{g}_h \end{pmatrix} =: F_h. \tag{10}$$

By construction $\tilde{A}$ is symmetric and a straightforward calculation shows that

$$\tilde{A} = (\mathrm{Id} - B^TW^T)A(\mathrm{Id} - WB) + B^TW^TAWB.$$

We recall that $B(\mathrm{Id} - WB) = 0$ and thus $(\mathrm{Id} - WB)v$ is an element of $\ker B_h$. Moreover, A restricted on $\ker B_h$ and $S_h := WBX_h$ is positive definite, see [5]. The decomposition $X_h = \ker B_h \oplus S_h$ is direct and each $v_h \in X_h$ can be uniquely decomposed into $v_h = v_0 + v_1$, $v_0 \in \ker B_h, v_1 \in S_h$. Then it is easy to see that $v_h\tilde{A}v_h = v_0Av_0 + v_1Av_1$, and thus $\tilde{A}$ is positive definite on X_h.

Lemma 3. *The saddle point problem* (5) *for* (u_h, λ_h) *and the positive definite system* (10) *for* u_h *together with the post-processing step* (8) *are equivalent.*

The proof follows by construction. We note that the matrix $\tilde{A}$ has exactly the same form as in a standard mortar problem with dual Lagrange multipliers. The interface conditions enter only into the right side F_h. Using the block decomposition of u_h, the matrix $\tilde{A}$ is a 3×3 block matrix. Now, we set $\tilde{M} := M_m^TD^{-1}$, and the third block of (10), $(0, A_{ss}\tilde{M}^T, A_{ss})$ can be multiplied from the left by A_{ss}^{-1}, and we obtain the non-symmetric system

$$\hat{A}u_h = \hat{F}_h, \tag{11}$$

where

$$\hat{A} = \begin{pmatrix} A_{ii} & A_{im} - A_{is}\tilde{M}^T & 0 \\ A_{mi} - \tilde{M}A_{si} & A_{mm} - \tilde{M}A_{sm} - A_{ms}\tilde{M}^T + 2\tilde{M}A_{ss}\tilde{M}^T & \tilde{M}A_{ss} \\ 0 & \tilde{M}^T & \mathrm{Id} \end{pmatrix}$$

and the right side can be written as

$$\hat{F}_h = \begin{pmatrix} \tilde{f}_i - A_{is}D^{-1}\tilde{g}_h \\ \tilde{f}_m - \tilde{M}f_s - A_{ms}D^{-1}\tilde{g}_h + 2\tilde{M}A_{ss}D^{-1}\tilde{g}_h \\ D^{-1}\tilde{g}_h \end{pmatrix}.$$

The third row of the right side $\hat{F}_h$ is $D^{-1}\tilde{g}_h$, and $\tilde{g}_h$ depends only on the given jump g_D at the interface. Our numerical computation is based on this non-symmetric system (11). We observe that the matrix $\hat{A}$ is exactly the same as in a mortar case without the jump terms, see [19]. Only the right side has a different form. Defining $\tilde{u}_h := u_h - (0, 0, D^{-1}\tilde{g}_h)^T$, we find that $\hat{A}\tilde{u}_h = \tilde{F}_h$, where $(\tilde{F}_h)_s = 0$, $(\tilde{F}_h)_m = (\hat{F}_h)_m - \tilde{M}A_{ss}D^{-1}\tilde{g}_h$ and $(\tilde{F}_h)_i = (\hat{F}_h)_i$. Thus the right side $\tilde{F}_h$ has exactly the same structure as in the standard mortar setting. To solve the problem $\hat{A}\tilde{u}_h = \tilde{F}_h$, we can apply the modified multigrid approach as discussed in [19], and use one local post-processing step to obtain $u_h = \tilde{u}_h + (0, 0, D^{-1}\tilde{g}_h)^T$.

Remark 4. *Applying a Gauß–Seidel smoother to $\hat{A}u_h = \hat{F}_h$, the third block component of the residual is zero after one smoothing step. In that case, we do not have to carry out the post-process. The structure of the smoother guarantees that the weak discrete form of* (2) *is automatically satisfied within the multigrid approach.*

4 Numerical results

Here, we present some numerical examples illustrating the flexibility and efficiency of the mortar finite element method with dual Lagrange multipliers to treat interface problems. All our numerical examples are realized within the finite element toolbox ug, [2]. We present the numerical results for various types of interface problems using linear and quadratic mortar finite elements. We denote by M_h^q and M_h^l the discontinuous dual Lagrange multiplier spaces for quadratic and linear finite elements, respectively, see [18]. In the case of M_h^q, the basis functions are piecewise quadratic, whereas the basis functions of M_h^l are piecewise linear. The mortar finite element solutions associated with the different Lagrange multiplier spaces M_h^q and M_h^l are denoted by u_h^q and u_h^l, respectively. For all our numerical examples, we use uniform refinement. The error in the Lagrange multipliers is measured in a mesh-dependent L^2-norm

$$\|\lambda_h\|_h^2 := \sum_{e \in \mathcal{T}_\Gamma} h_e \|\lambda_h\|_{0;e}^2, \tag{12}$$

where h_e is the length of the edge e on the slave side. For the first three examples, we take the domain $\Omega = (-1, 1) \times (0, 1)$ decomposed into two squares $\Omega_1 = (-1, 0) \times (0, 1)$ and $\Omega_2 = (0, 1) \times (1, 0)$ with the interface $\Gamma = \{0\} \times (0, 1)$. The initial non-matching triangulation and the decomposition into the two subdomains are shown in the left picture of Figure 4.

Our first four examples are based on the interface problem

$$\begin{aligned} -\Delta u &= f \quad \text{in} \quad \Omega \quad \text{with} \quad u_{|\partial\Omega} = g, \\ [u]_n &= g_N \quad \text{and} \quad [u] = g_D. \end{aligned}$$

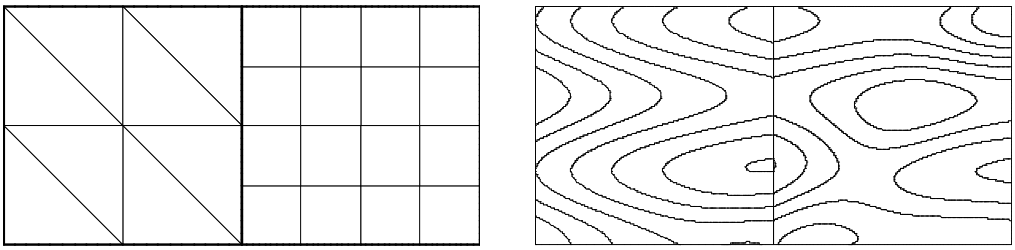

Figure 4: Decomposition into two subdomains and initial triangulation for Examples 1-3 (left) and isolines of the solution for Example 1 (right)

Different jumps g_D in the trace and jumps g_N in the flux are considered. We start with an example given by the exact solution

$$\begin{aligned} u_1(x,y) &= \exp(-10(x-y)^2)\cos(x^2+2y^2) + \sin(2x) + \cos(10y) - 4x, \\ u_2(x,y) &= (x+1)\exp(-10(x-y)^2)\cos(x^2+2y^2) + \sin(2x) + \cos(10y). \end{aligned}$$

It is easy to see that $[u] = 0$ on Γ and thus $g_D = 0$. Here, the flux at the interface Γ is $g_N = -4 - \exp(-10\,y^2)\cos(2\,y^2)$. The isolines of the solution are shown in the right picture of Figure 4. In Figure 5, we show the discretization errors in different norms versus the number of elements. In particular, we consider the errors in the L^2- and H^1-norm for the solution and for the flux in a mesh-dependent L^2-norm as defined by (12). The numerical results confirm the theoretical ones. In the L^2-norm, the error decay is of order h^2 for the linear case and of order h^3 for the quadratic case. The error in the H^1-norm is of order h and h^2. Since the solution is smooth, we obtain better results for the error in the flux. Asymptotically, the error in the energy norm is distributed equally. Thus the error of the flux in the mesh-dependent norm is of order $h^{3/2}$ and of order $h^{5/2}$ for the linear and the quadratic case, respectively.

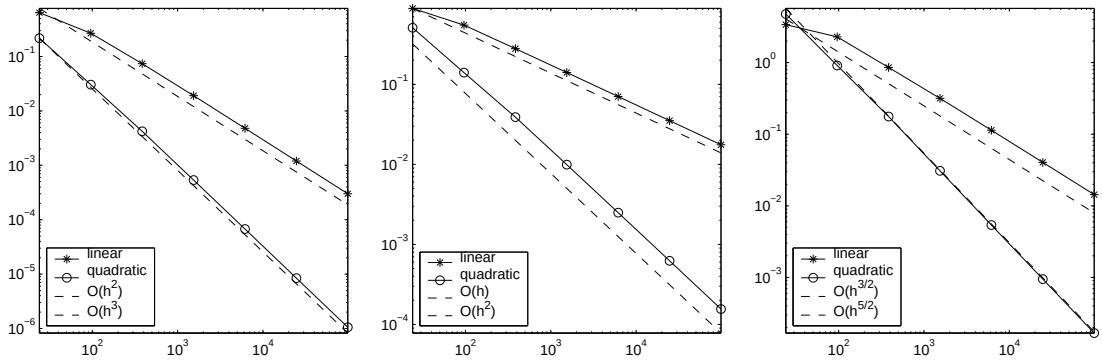

Figure 5: Error plot versus number of elements, L^2-norm (left), H^1-norm (middle) and weighted Lagrange multiplier norm (right), (Example 1)

In our second example, we consider a problem with non-vanishing jump in the solution but vanishing jump in the normal derivative on the interface. The exact solution is set to be

$$\begin{aligned} u_1(x,y) &= (1-y^2)\sin(12x^2+y), \\ \text{and} \quad u_2(x,y) &= 2-(1+y^2)\sin(12x^2+y). \end{aligned}$$

Then, the jump of the solution at the interface Γ is given by $g_D = 2\sin(y) - 2$, and the jump of the flux on the interface Γ is zero. The isolines of the solution are shown in the left picture of Figure 7. The error decay in different norms is given in Figure 6. As in Example 1, the numerical results for the discretization errors confirm the theory. Almost from the beginning, the correct asymptotic rates can be observed.

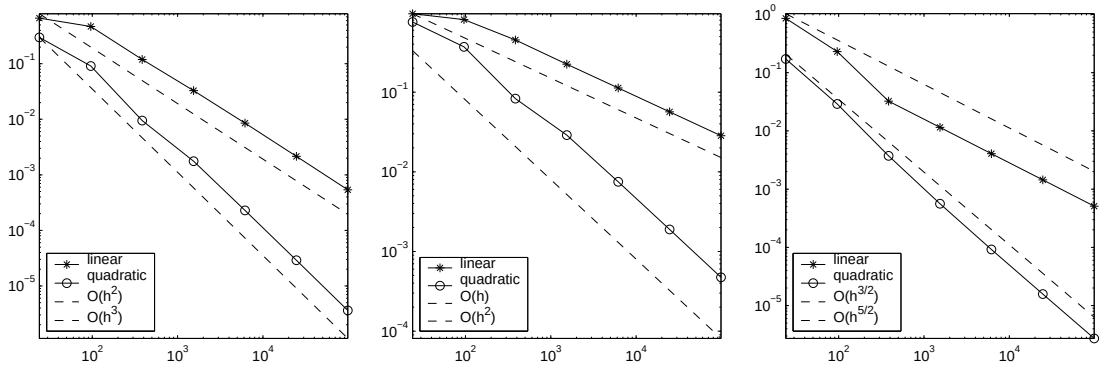

Figure 6: Error plot versus number of elements, L^2-norm (left), H^1-norm (middle) and weighted Lagrange multiplier norm (right), (Example 2)

In the third example, we consider a problem with a jump in the trace as well as in the flux. In this example, both g_D and g_N are non-zero. The exact solution is given by

$$\begin{aligned} u_1(x,y) &= (x^2+y^2+1)\cos(x+12y), \\ \text{and} \quad u_2(x,y) &= (x^2+y^2)\cos(x+12y)+1. \end{aligned}$$

Here, we find $g_D = \cos(12y) - 1$ and $g_N = \sin(12y)$. In the right picture of Figure 7, the isolines of the solution are shown.

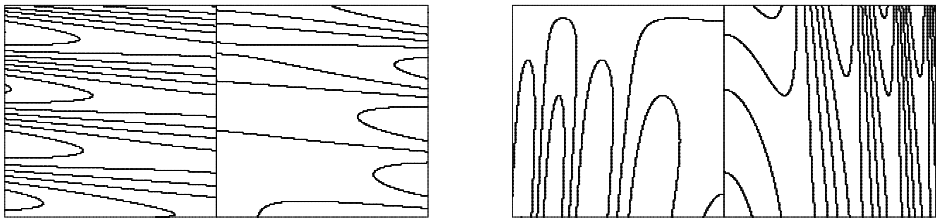

Figure 7: Isolines of the solution, Example 2 (left) and Example 3 (right)

The discretization errors are given in Figure 8. As before, the numerical results confirm the theoretical ones.

In the following two examples, we use a different decomposition of $\bar{\Omega} = \bar{\Omega}_1 \cup \bar{\Omega}_2$, where $\Omega = (0,2) \times (0,1)$. Here, $\Omega_2 = (0.5, 1.5) \times (0.25, 0.75)$, and Ω_1 is a non-convex subdomain given by $\Omega_1 = \Omega \backslash \bar{\Omega}_2$, see Figure 9. We note that Γ can be decomposed into four straight segments, γ_l, $1 \le l \le 4$. The corner nodes of Ω_2 are crosspoints and they do not carry a degree of freedom for the Lagrange multiplier space.

In Example 4, we consider the Poisson equation $-\Delta u = f$, where the exact solution is given

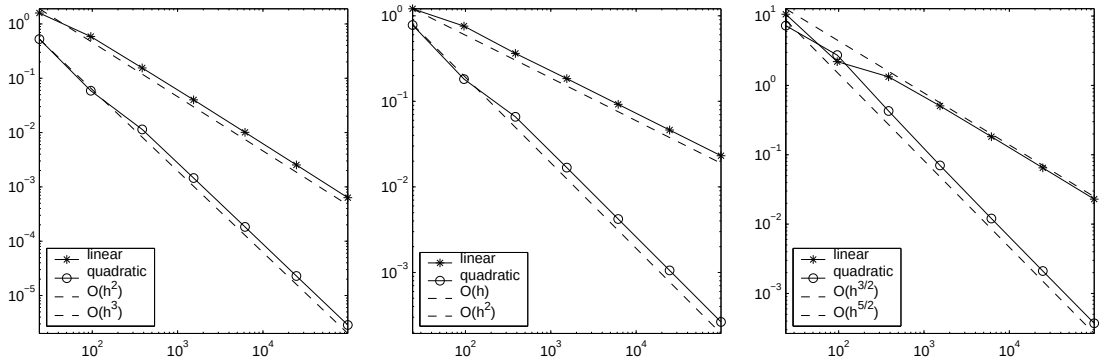

Figure 8: Error plot versus number of elements, L^2-norm (left), H^1-norm (middle) and weighted Lagrange multiplier norm (right), (Example 3)

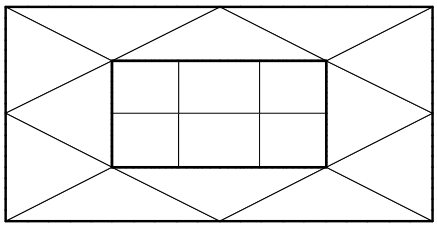

Figure 9: Decomposition of the domain and initial triangulation for Examples 4 and 5

by

$$\begin{aligned} u_1(x,y) &= \exp(-a_1(y-0.5)^2)(\cos(x+y))^2, \\ \text{and} \quad u_2(x,y) &= \exp(-a_2((x-1)^2+(y-0.5)^2)) \end{aligned}$$

with $a_1 = 12$ and $a_2 = 10$. As before, the right side f, the jump in the solution g_D and the jump in the flux g_N are defined by the exact solution. We note that $g_N \notin H^{1/2}(\Gamma)$, but $g_N \in H^{1/2}(\gamma_l)$, $1 \le l \le 4$. The isolines of the numerical solution are shown in the left picture of Figure 11. The discretization errors are given in Figure 10.

In our Example 5, we consider the problem

$$-\mathrm{div}(\alpha \nabla u) + bu = f \quad \text{in} \quad \Omega \quad \text{with} \quad u_{|\partial\Omega} = g,$$

$$[u]_n = g_N \quad \text{and} \quad [u] = g_D.$$

We use a discontinuous diffusion tensor α, which is defined as

$$\begin{pmatrix} 2.5 & 0 \\ 0 & 1 \end{pmatrix} \quad \text{and} \quad \begin{pmatrix} 1 & 0 \\ 0 & 2.5 \end{pmatrix}$$

in the first and second subdomain, respectively. Similarly, we choose a discontinuous b to be defined as $b(x,y) := x^2 + y^2 + xy$ in the first subdomain and $b(x,y) := 0$ in the second subdomain. We set the exact solution to be

$$\begin{aligned} u_1(x,y) &= \sin(x^2+y)\exp(-(x-y)^2), \\ \text{and} \quad u_2(x,y) &= 1.5\exp(-(x-1)^2-(y-0.5)^2). \end{aligned}$$

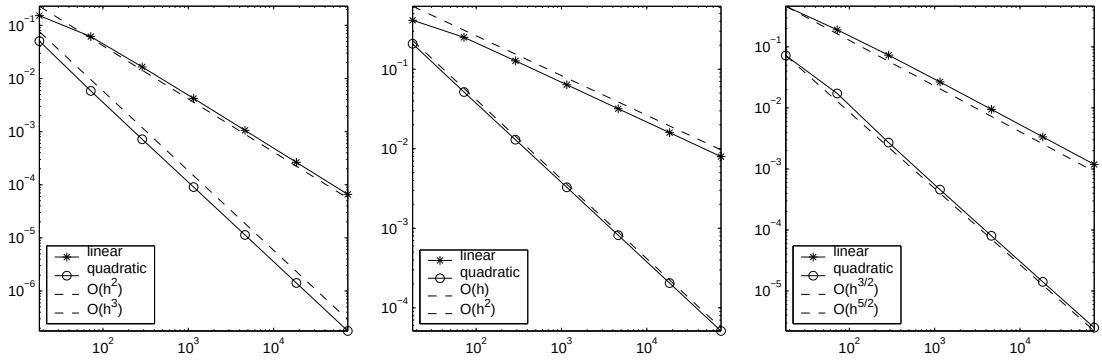

Figure 10: Error plot versus number of elements, L^2-norm (left), H^1-norm (middle) and weighted Lagrange multiplier norm (right), (Example 4)

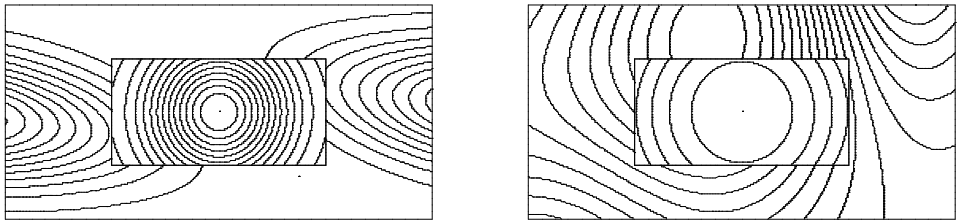

Figure 11: Isolines of the solution, Example 4 (left) and Example 5 (right)

The isolines of the solution are given in the right picture of Figure 11 and the discretization errors are shown in Figure 12. Examples 4 and 5 show the same asymptotic rates as the first three examples. Having a decomposition where Γ is not a straight lines does not influence the convergence rates. In contrast to mortar techniques with many subdomains, we do not have to reduce the dimension of the Lagrange multiplier space at the crosspoints because of the inf-sup condition. The inf-sup condition is also satisfied for the higher dimensional space $\tilde{M}_h$, where $\tilde{M}_h$ is spanned by the biorthogonal basis functions associated with all nodes including the crosspoints on the slave side. However, replacing the Lagrange multiplier space M_h by $\tilde{M}_h$ yields considerably worse numerical results for the discretization error in the Lagrange multiplier. This is due to the fact that λ is not in $H^{1/2}(\Gamma)$ and that $\tilde{M}_h$ does not contain the constants per straight segment γ_l.

In our last example, we consider a problem with a corner singularity. Here, we decompose the unit square into two subdomains Ω_1 and Ω_2. The subdomain Ω_1 is a L-shape domain and $\Omega_2 = (0.5, 1) \times (0, 0.5)$, see the left picture of Figure 13. The initial triangulations do not match at the interface. The problem for this example is given by $-\Delta u = f$, and the exact solution is chosen as $u_1 = r^{2/3} \sin(\frac{2\phi}{3})$ and $u_2 = r^2$. Here, (r, ϕ) are the polar coordinates with origin shifted to $(0.5, 0.5)$. The isolines of the solution are shown in the right picture of Figure 13.

Here, the solution is not piecewise H^2-regular, and asymptotically we cannot expect the same order of convergence as in the other examples. We note that g_N is a L^2-function. The errors in the L^2-, H^1- and the weighted Lagrange multiplier norms are given in Table 1. Here we use lowest order finite elements. Asymptotically, we expect an order $h^{2/3}$ for the

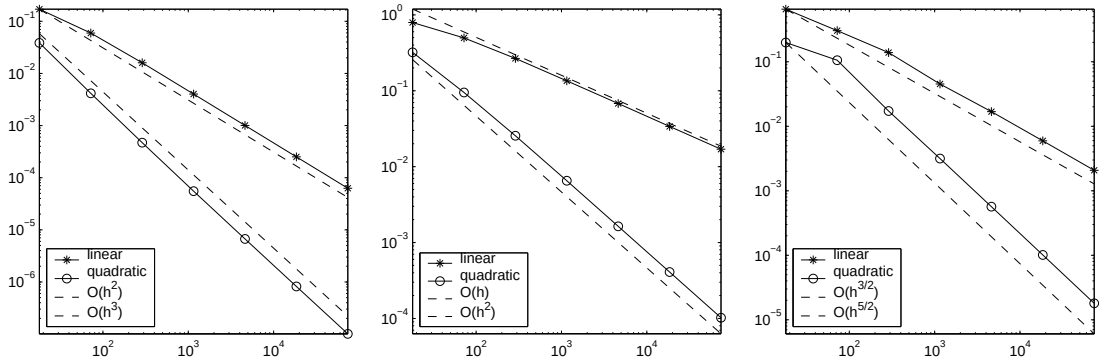

Figure 12: Error plot versus number of elements, L^2-norm (left), H^1-norm (middle) and weighted Lagrange multiplier norm (right), (Example 5)

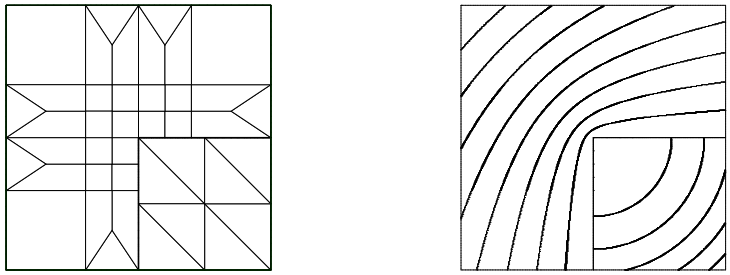

Figure 13: Decomposition into two subdomains and initial triangulation (left), isolines of the solution (right), (Example 6)

H^1-norm which can be observed. We note that the convergence rates are considerably better in the beginning. In contrast to our other examples, the Lagrange multiplier does not show a better asymptotic convergence rate. Asymptotically, we obtain the same convergence rate as in the H^1-norm. This is due to the concentration of the error at the point $(0.5, 0.5)$ which is located on the interface. Better convergence rates can be observed if the solution has no singularity at the interface.

Table 1: Discretization errors in the L^2-, H^1- and weighted Lagrange multiplier norm (Example 6)

level	# elem.	$\|u-u_h^l\|_0$	ratio	$\|u-u_h^l\|_1$	ratio	$\|\lambda-\lambda_h^l\|_h$	ratio
0	41	3.325808e-02		1.370511e-01		1.667159e-02	
1	164	8.446641e-03	3.9374	7.408534e-02	1.8499	4.399131e-03	3.7897
2	656	2.122112e-03	3.9803	4.111530e-02	1.8019	1.584474e-03	2.7764
3	2624	5.335827e-04	3.9771	2.343380e-02	1.7545	7.218470e-04	2.1950
4	10496	1.348615e-04	3.9565	1.369342e-02	1.7113	3.889129e-04	1.8561
5	41984	3.434135e-05	3.9271	8.173967e-03	1.6752	2.289971e-04	1.6983
6	167936	8.837528e-06	3.8859	4.961475e-03	1.6475	1.403140e-04	1.6320
7	671744	2.307613e-06	3.8297	3.048681e-03	1.6274	8.741203e-05	1.6052

References

[1] Babuška, I. The finite element method for elliptic equations with discontinuous coefficients. *Computing 5* (1970), 207–213.

[2] Bastian, P., Birken, K., Johannsen, K., Lang, S., Neuss, N., Rentz–Reichert, H., and Wieners, C. UG – a flexible software toolbox for solving partial differential equations. *Computing and Visualization in Science 1* (1997), 27–40.

[3] Becker, R., Hansbo, P., and Stenberg, R. A finite element method for domain decomposition with non-matching grids. *Preprint 2001-15, Chalmers University of Technology, Goetborg, Sweden* (2001). to appear in M^2AN.

[4] Belgacem, F. B. The mortar finite element method with Lagrange multipliers. *Numer. Math. 84* (1999), 173–197.

[5] Bernardi, C., Maday, Y., and Patera, A. Domain decomposition by the mortar element method. In *In: Asymptotic and numerical methods for partial differential equations with critical parameters* (1993), H. K. et al., Ed., Reidel, Dordrecht, pp. 269–286.

[6] Bernardi, C., Maday, Y., and Patera, A. A new nonconforming approach to domain decomposition: the mortar element method. In *In: Nonlinear partial differential equations and their applications* (1994), H. B. et al., Ed., Paris, pp. 13–51.

[7] Braess, D. *Finite Elements. Theory, fast solver, and applications in solid mechanics.* Cambridge Univ. Press, Second Edition, 2001.

[8] Bramble, J., and King, J. A finite element method for interface problems in domains with smooth boundaries and interfaces. *Adv. Comput. Math. 6* (1996), 109–138.

[9] Cao, Y., and Gunzburger, M. Least-squares finite element approximations to solutions of interface problems. *SIAM J. Numer. Anal. 35* (1998), 393–405.

[10] Chen, Z., and Zou, J. Finite element methods and their convergence for elliptic and parabolic interface problems. *Numer. Math. 79* (1998), 175–202.

[11] Hansbo, A., and Hansbo, P. An unfitted finite element method, based on Nitsche's method, for elliptic interface problems. *Comput. Methods Appl. Mech. Engrg. 191* (2002), 5537–5552.

[12] Heinrich, B., and Nicaise, S. Nitsche mortar finite element method for transmission problems with singularities. *Preprint SFB393/01-10, TU Chemnitz* (2001).

[13] Huang, J., and Zou, J. Some new a priori estimates for second-order elliptic and parabolic interface problems. *J. Differ. Equations 184* (2002), 570–586.

[14] LeVeque, R., and Li, Z. The immersed interface method for elliptic equations with discontinuous coefficients and singular sources. *SIAM. J. Numer. Anal. 31* (1994), 1019–1044.

[15] Li, Z. A fast iterative algorithm for elliptic interface problems. *SIAM. J. Numer. Anal. 35* (1998), 230–254.

[16] Li, Z. The immersed interface method using a finite element formulation. *Appl. Numer. Math. 27* (1998), 253–267.

[17] Wiegmann, A., and Bube, K. The explicit-jump immersed interface method: Finite difference methods for pdes with piecewise smooth solutions. *SIAM J. Numer. Anal. 37* (2000), 827–862.

[18] Wohlmuth, B. *Discretization Methods and Iterative Solvers Based on Domain Decomposition*, vol. 17 of *LNCS*. Springer Heidelberg, 2001.

[19] Wohlmuth, B., and Krause, R. Multigrid methods based on the unconstrained product space arising from mortar finite element discretizations. *SIAM J. Numer. Anal. 39* (2001), 192–213.

[20] Xu, J., and Zou, J. Some non-overlapping domain decomposition methods. *SIAM Review 40* (1998), 857–914.

Bishnu P. Lamichhane

Universität Stuttgart
Pfaffenwaldring 57
70569 Stuttgart
Germany

E-Mail: lamichhane@mathematik.uni-stuttgart.de

WWW: http://www.mathematik.uni-stuttgart.de/mathA/lst7/lamichhane/lamichhane.shtml

Barbara I. Wohlmuth

Universität Stuttgart
Pfaffenwaldring 57
70569 Stuttgart
Germany

E-Mail: wohlmuth@mathematik.uni-stuttgart.de

WWW: http://www.mathematik.uni-stuttgart.de/mathA/lst7/wohlmuth/wohlmuth.shtml

Erschienene Preprints ab Nummer 2003/001

Komplette Liste: `http://preprints.ians.uni-stuttgart.de`

2003/001 *Lamichhane, B. P., Wohlmuth, B. I.*: Mortar Finite Elements for Interface Problems